New Method to Determine PSD Using Supercritical Adsorption: Applied to Methane Adsorption in Activated Carbon

ARTICLE *in* LANGMUIR · SEPTEMBER 2006

Impact Factor: 4.46 · DOI: 10.1021/la061079+ · Source: PubMed

2 AUTHORS:

Greg R. Birkett
University of Queensland
31 PUBLICATIONS **212** CITATIONS
SEE PROFILE

Duong Do
University of Queensland
493 PUBLICATIONS **9,807** CITATIONS
SEE PROFILE

New Method to Determine PSD Using Supercritical Adsorption: Applied to Methane Adsorption in Activated Carbon

G. Birkett and D. D. Do*

Department of Chemical Engineering, University of Queensland, St. Lucia, Qld 4072, Australia

Received April 21, 2006. In Final Form: June 8, 2006

Adsorption of supercritical fluids is increasingly carried out to determine the micropore size distribution. This is largely motivated by the advances in the use of supercritical adsorption in high energy applications, such as hydrogen and methane storage in porous media. Experimental data are reported as mass excess versus pressure, and when these data are matched against the theoretical mass excess, significant errors could occur if the void volume used in the calculation of the experimental mass excess is incorrectly determined [Malbrunot, P.; Vidal, D.; Vermesse, J.; Chahine, R.; Bose, T. K. *Langmuir* **1997**, *13*, 539].[1] The incorrect value for the void volume leads to a wrong description of the maximum in the plot of mass excess versus pressure as well as the part of the isotherm over the pressure region where the isotherm is decreasing. Because of this uncertainty in the maximum and the decreasing part of the isotherm, we propose a new method in which the problems associated with this are completely avoided. Our method involves only the relationship between the amount that is introduced into the adsorption cell and the equilibrium pressure. This information of "direct" experimental data has two distinct advantages. The first is that the data is the "raw" data without any manipulation (i.e., involving further calculations), and the second one is that this relationship always monotonically increases with pressure. We will illustrate this new method with the adsorption data of methane in a commercial sample of activated carbon.

1. Introduction

One of the most important physical characteristics of a porous solid in adsorption studies is the pore size distribution (PSD).[2−8] This information is traditionally obtained with adsorption methods such as adsorption of nitrogen and argon at their respective boiling points. To apply these data, theoretical isotherms have to be obtained and matched against the data to obtain the pore size distribution. The theoretical isotherms can be calculated with classical tools, such as BET equations, Dubinin equations, Kelvin−Cohan equations, etc. However, in recent years, this is achieved with more accurate molecular simulation tools, such as Monte Carlo[9] (MC), molecular dynamics,[9] and density functional theory.[10,11] These tools provide more accurate local isotherms in pores without the need to combine the various mechanisms of adsorption as traditionally done in the classical theories. No matter whether we use the classical theories or molecular simulation tools, theoretical isotherms and the subsequent derivation of pore size distribution can only be obtained after we have made the following assumptions: (1) pore model (shape, size, topology, etc.), (2) mechanism of adsorption (applied to classical theories only), and (3) correct branch of the isotherm (if there is hysteresis) to be used.

To obtain a local isotherm of a single pore, one has to assume its pore structure: shape, size, and the chemistry of the surface. The choice of the complexity of a solid model depends on the balance on how much we know about it and the need to make it simple so that the computation time is not excessive. The simplest model is a well-defined pore shape, such as a slit pore of infinite extent in two lateral directions or a uniformly sized cylindrical pore of infinite extent along the pore axis. For activated carbon, the porous solid is generally assumed to be composed of stacks of graphene layers leading to the classical slit pore geometry. This is the model most often used in the literature. The reason for this choice is purely on the computation time rather than an unwillingness to model it in a more complex way.

As stated, molecular simulations are now preferred over classical techniques due to accuracy and indiscriminate applicability for generating theoretical isotherms for different model pores. However, even with the application of the powerful molecular simulation methods, one is still faced with the distinct adsorption−desorption branches. For the simplest homogeneous pore of infinite extent, this distinction is usually attributed to the meta-stability of the system. Experimentally, we also observe distinct adsorption−desorption branches. Traditionally, it has been assumed that the experimental desorption branch is the equilibrium one and the equilibrium theoretical isotherm must be obtained to match it against the experimental one. This poses a serious problem. How does one justify that the experimental desorption branch is the equilibrium branch? Could it be due the pore blocking effects? This is a complex issue associated with the adsorption of fluid under subcritical conditions.

If our interest is to determine the micropore size distribution, where the majority of adsorption capacity resides for many solids, we can carry out adsorption measurements under supercritical conditions. The advantage of doing this is that there is no hysteresis as the adsorption temperature is above the hysteresis temperature. Although we overcome the problem of adsorption−desorption hysteresis by using supercritical fluids, the principle problem associated with supercritical adsorption is that the pressure

* To whom correspondence should be addressed. Tel: +61-7-3365-4154. Fax: +61-7-3365-2789. E-mail: duongd@cheque.uq.edu.au.

(1) Malbrunot, P.; Vidal, D.; Vermesse, J.; Chahine, R.; Bose, T. K. *Langmuir*. **1997**, *13*, 539.
(2) Kaneko, K. *J. Membr. Sci.* **1994**, *96*, 59.
(3) Heuchel, M.; Jaroniec, M. *Langmuir* **1995**, *11*, 4532.
(4) Krak, M.; Jaroniec, M.; Gadkaree, K. P. *Langmuir* **1992**, *15*, 1442.
(5) Li, Z.; Kruk, M.; Jaroniec, M.; Ryn, S. *J. Colloid Interface Sci.* **1998**, *204*, 151.
(6) Ohba, T.; Kaneko, K. *Langmuir* **2001**, *17*, 3666.
(7) Garalda, S.; Gubbins, K.; Hanzalsa, Y.; Kaneko, K.; Thomson, K. T. *Langmuir* **2002**, *18*, 2141.
(8) Ohba, T.; Nicholson, D.; Kaneko, K. *Langmuir* **2003**, *19*, 5700.
(9) Allen, M. P.; Tildesley, D. J. *Computer Simulation of Liquids*; Clarendon Press: Oxford, 1987. Nicholson, D.; Parsonage, N. G. *Computer Simulation and the Statistical Mechanics of Adsorption*; Academic Press: London, 1982.
(10) El-Merraoui, M.; Aoshima, M.; Kaneko, K. *Langmuir* **2000**, *16*, 4300.
(11) Tanaka, H.; El-Merraoui, M.; Kodaira, T.; Kaneko, K. *Chem. Phys. Lett.* **2002**, *351*, 417.

10.1021/la061079+ CCC: $33.50
Published on Web 08/01/2006

required is usually very high (at least on the order of 200 atm to yield acceptable pore size distribution). Notwithstanding these problems, attempts to calculate pore size distributions from supercritical data have been attempted in the literature.[12−14] These have shown that reasonable pore size distributions can be achieved which fit the adsorption of the supercritical fluid very well. It has also been shown that a pore size distribution fitting subcritical data can result in extremely erroneous predictions of adsorption at supercritical conditions.[12] Another problem with using supercritical data is that the calculated isotherm in terms of mass excess which, if the void volume is not obtained correctly, can lead to significant errors in the experimental isotherms.[1] This in turn leads to incorrect pore size distributions. In this paper, we will present a new method of determining the pore size distribution using supercritical fluids without the need to use the void volume. Our method involves only direct measurable quantities. We will illustrate this method with methane adsorption in activated carbon.

2. Relationship between Experiment, Simulation, and the PSD

2.1. Experimental Excess Adsorption. Let us deal with the conventional volumetric method. In this method, the adsorption cell of volume V is composed of the volume of the bulk phase, the void volume of the solid particles, and the solid volume. With this definition, it does not mean that we have to clearly define the demarcation between the bulk volume and the void volume of the particles. The solid volume would encompass the closed void volume embedded within the solid.

To obtain the total void volume which includes the bulk volume and the solid's void volume, the helium expansion method is traditionally carried out. With the introduction of N moles of helium from a reservoir of known volume into the adsorption cell and knowing the pressures before and after expansion, the total void volume can be obtained by assuming (1) ideal gas behavior and (2) helium does not adsorb inside the pores. The first assumption is satisfied for helium at ambient conditions, whereas the second one requires some consideration of the solid under investigation. If the solid does not contain any small micropores, then the second assumption is satisfied because helium does not adsorb in mesopores and larger (strictly speaking, it does but in a negligible quantity). However, when the solid contains fine micropores such as microporous activated carbon, there is a possibility that helium will adsorb in those pores even at ambient conditions. Thus, there is a risk in using the helium expansion method to determine the void volume if we do not know the details of the porous structure (Appendix 1).

To overcome the problems associated with the helium expansion method. We suggest that the void volume be determined directly from the analysis of adsorption data rather than requiring a separate experiment of helium expansion. This will be done in Section 3. Before we do this, it is important that we present physical and accessible pore volumes of pores of molecular dimension in an unambiguous manner.

2.2. Accessible Pore Volume and Width. The accessible pore volume is defined as the volume in which a particle can be probed. The boundary of this accessible volume is defined as the loci of positions at which the solid−fluid potential between a particle and the pore is zero. If the distance from one of the pore walls to the center of a molecule at which the solid−fluid potential is zero is z_0, the accessible pore width is

$$H' = (H - 2z_0 + \sigma) \tag{1}$$

where H is the physical width of the pore, which is defined as the distance from the plane passing through all carbon atoms of the outermost layer of one wall to the corresponding plane of the opposite wall, and σ is the collision diameter of that closest site. This formula was suggested by Everett and Powl[15] and Kaneko et al.[16] The distance z_0 would depend on the physical pore width due to energy contributions from the opposing surface. Accessible pore widths, for a range of physical pore widths, have been listed in Appendix 2.

2.3. Absolute and Excess Pore Density. Since the local particle density varies with position within a pore, the density that is reported and presented in the isotherm is the average pore density, which is defined as the number of particles per unit volume. Therefore, its definition depends on the choice of the volume. With the definition of the accessible pore width as presented above, we can define the average pore density in two ways. We can use either the physical pore volume (AH) or the accessible pore volume (AH'), and so these two average densities are

$$\langle\rho\rangle = \frac{\langle N\rangle}{AH}; \quad \langle\rho\rangle' = \frac{\langle N\rangle}{AH'} \tag{2}$$

where $\langle N\rangle$ is the ensemble average of the number of particle in the simulation box, A is the area of one wall of the pore, and H and H' are the physical and accessible pore widths, respectively. The plot of either $\langle\rho\rangle$ or $\langle\rho\rangle'$ versus pressure is the absolute adsorption isotherm at a given temperature, whereas the plot of $\langle\rho\rangle' - \rho_b$ versus pressure is the excess adsorption isotherm because $V'\langle\rho\rangle'$ is the number of mole of adsorbate in the pore and $V'\rho_b$ is the theoretical number of mole of adsorbate if the density in the pore is the same the density of the bulk phase. It is the latter that is measured experimentally as we show in the next section.

2.4. Determination of Pore Size Distribution and External Surface Area. We have defined the accessible pore width, the accessible pore volume, and two definitions of pore density. Now we turn to a new method to determine the pore size distribution, and it is important to define it unambiguously in the same way that we did for volume and density. The pore size distribution is denoted as $f(H)$, with

$$\mathrm{d}V = f(H)\,\mathrm{d}H \qquad [\mathrm{m}^3/\mathrm{kg}] \tag{3}$$

being the differential specific physical volume of pores having physical widths falling in the range between H and $H + dH$. Here we use the unambiguous physical pore width in the definition of the pore size distribution as the accessible pore width depends on the adsorbate. If we know the physical pore volume, the differential accessible pore volume in this range is calculated from

$$\mathrm{d}V' = \frac{H'}{H} f(H)\,\mathrm{d}H \tag{4}$$

We use the prime to denote the excess or accessible quantities. The specific physical and accessible pore volumes (m^3/kg) are the integration of the above equation from 0 to infinity (this upper limit means to include the space outside the particle)

(12) Sweatman, M. B.; Quirke, N. *Langmuir* **2001**, *17*, 5011.
(13) Sweatman, M. B.; Quirke, N. *J. Phys. Chem. B* **2001**, *105*, 1403.
(14) Sweatman, M. B.; Quirke, N. *J. Phys. Chem. B* **2005**, *109*, 10381.
(15) Everett, D.; Powl, J. *J. Chem. Soc. Faraday Trans.* **1976**, *72*, 619.
(16) Kaneko, K.; Cracknell, R.; Nicholson, D. *Langmuir* **1994**, *10*, 4606

$$V = \int_0^\infty f(H)\,\mathrm{d}H; \quad V' = \int_0^\infty \frac{H'}{H} f(H)\,\mathrm{d}H \tag{5}$$

Let ρ_{av} (which is equivalent to $\langle\rho\rangle$ obtained from the Monte Carlo simulation) be the average pore density based on the physical pore volume in pores of width H. This average pore density is a function of pressure (P) and the physical pore width (H). Thus, for a system containing a range of physical pore widths from 0 to infinity, the number of mole in the adsorption system containing m_p (kg) of particles is

$$N = m_p \int_0^\infty \rho_{av}(P;H)\,\mathrm{d}V \qquad [\mathrm{mol}] \tag{6}$$

Let us subtract and add to the right-hand side of the above equation with $m_p V' \rho_b$, which is simply the hypothetical number of mole in the system if the void accessible volume, V' (including space outside the particles), is filled with gas at the bulk density. This void volume is specific to the adsorbate under consideration and it might not be the same as the void volume for another adsorbate. The above equation can be rewritten as

$$N = m_p\left[\int_0^\infty \rho_{av}(P;H)\,\mathrm{d}V - \int_0^\infty \rho_b\,\mathrm{d}V'\right] + m_p V' \rho_b \tag{7}$$

Rearranging the above equation, we get

$$\frac{N - m_p V' \rho_b}{m_p} = \int_0^\infty \rho_{av}(P;H)\,\mathrm{d}V - \int_0^\infty \rho_b\,\mathrm{d}V' \tag{8}$$

As always done in all experiments, the void volume, V', is taken to be the void volume obtained with helium expansion (V'_{He}) and it was recommended that this should be measured at high temperature to avoid the possibility of helium adsorption in fine pores. The problem of using this relation $V' = V'_{He}$ lies in the fact that in general we would expect that $V' \neq V'_{He}$ because of not only the difference in the collision diameter and the well-depth of solid−fluid interaction energy of helium compared to the corresponding quantities of the adsorbate under consideration but also on the possibility that helium can access to the pore spaces that the adsorbate cannot. However, if one formally proceeds with the use of the void volume measured with the helium expansion method, the left-hand side of eq 8 is the quantity that one would use to calculate the "experimental" mass excess, which is simply the difference between the amount dosed into the system and the amount that is left in the bulk phase. We need to stress here that this quantity is a calculated one, not a direct experimental data. The error of this calculation would magnify greatly if the bulk gas density is comparable to the adsorbed density, and this is exactly the case at high pressures in supercritical adsorption.

Rearranging the right-hand side of eq 8 by applying eq 4, we get

$$\frac{N - m_p V' \rho_b}{m_p} = \int_0^\infty \left[\rho_{av}(P;H) - \rho_b\left(\frac{H'}{H}\right)\right]\mathrm{d}V \tag{9}$$

We have mentioned earlier that the average pore density is not only a function of pressure but also of the pore width. Its dependence on pore width is significant for pores in the micropore and mesopore ranges, and it becomes much less significant for larger pores, especially under supercritical conditions. For large pores having a width greater than a threshold value H^*, there is no (or insignificant) enhancement in the solid−fluid potential, and therefore, the surface densities in those pores are practically the same. Thus, by splitting the above integral into two integrals for two different ranges of pore width, we have

$$\frac{N - m_p V' \rho_b}{m_p} = \int_0^{H^*} \left[\rho_{av}(P;H) - \rho_b\left(\frac{H'}{H}\right)\right]\mathrm{d}V + \int_{H^*}^\infty \left[\rho_{av}(P;H) - \rho_b\left(\frac{H'}{H}\right)\right]\mathrm{d}V \tag{10}$$

The second integral on the right-hand side of the above equation is simply the amount adsorbed on surfaces (see Appendix 3), and therefore, we can rewrite the above equation as

$$\frac{N - m_p V' \rho_b}{m_p} = \int_0^{H^*} \left[\rho_{av}(P;H) - \rho_b\left(\frac{H'}{H}\right)\right]\mathrm{d}V + \Gamma(P) S_{ext} \tag{11}$$

where $\Gamma(P)$ is the surface excess for surface adsorption (mol/m^2) and S_{ext} is the external surface area (m^2/kg) contributed by all pores having width greater than H^* (including the outside surface area of particles). This equation states that the amount adsorbed in particles consists of the excess amount in pores having widths less than H^* and the surface excess on external surfaces, formed by all pores having widths greater than H^*.

The surface excess is obtained from the GCMC simulation of a very large pore as follows:

$$\Gamma(P) = \frac{\langle N\rangle - AH'\rho_b}{2A} \tag{12}$$

whereas the average pore density (based on the physical pore volume) is obtained from the GCMC simulation as

$$\rho_{av} = \frac{\langle N\rangle}{AH} \tag{13}$$

The left-hand side of eq 11 is commonly reported in the literature as the amount adsorbed (excess quantity), and this amount adsorbed when plotted against pressure is known as the isotherm commonly reported in the literature. For supercritical adsorption and high enough pressure, this mass excess quantity decreases with pressure because the rate of increase of the amount adsorbed with respect to pressure is lower than the rate of increase in the bulk density. This is tantamount to saying that compression of molecules in the bulk phase (isotropic fluid) is more efficient than compressing the adsorbed molecules, and this is simply due to the greater fluid−fluid interaction than the solid−fluid interaction at very high pressures.

When we use the experimental isotherm to match against the GCMC simulation results, we have to minimize the difference between the experimental results (which is the left-hand side of eq 11) and the theoretical calculations of the right-hand side of eq 11. In doing this, we have to accept blindly the calculated experimental amount adsorbed. That means that we have to trust a value of the void volume, usually measured with the helium expansion method as we have mentioned earlier. Although it is reported that the measurements of void volume by using helium should be done at high temperatures to avoid adsorption of helium in small pores, there is no guarantee that we can eliminate completely the adsorption of helium in those pores and resolve the situation whereby helium may access regions where adsorbate molecules cannot. To avoid this uncertainty, we now introduce a new approach which completely removes these uncertainties. This approach is outlined below.

3. New Proposal

Since the amount introduced into the adsorption cell is known accurately, it is more convenient to report the adsorption data of supercritical conditions as the amount introduced into the adsorption cell (N) as a function of equilibrium pressure. So we rewrite eq 11 in the following form:

$$N = m_p\left\{\int_0^{H^*}\left[\rho_{av}(P;H) - \rho_b\left(\frac{H'}{H}\right)\right] dV + \Gamma(P)S_{ext}\right\} + m_p V'\rho_b \quad (14)$$

The void volume is the difference between the volume of the empty adsorption cell and the volume occupied by the solid, $m_p V' = V_{cell} - m_p/\rho_s$, where ρ_s is the solid density. Hence, the above equation becomes

$$N = m_p\left\{\int_0^{H^*}\left[\rho_{av}(P;H) - \rho_b\left(\frac{H'}{H}\right)\right] dV + \Gamma(P)S_{ext}\right\} + \left(V_{cell} - \frac{m}{\rho_s}\right)\rho_b \quad (15a)$$

We can write this equation in a slightly different form, in which we lump the terms involving the bulk density together as follows:

$$N = m_p\{\int_0^{H^*} \rho_{av}(P;H)\, dV + \Gamma(P)S_{ext}\} + V''\rho_b \quad (15b)$$

where the new volume V'' is given by

$$V'' = \left[\left(V_{cell} - \frac{m_p}{\rho_s}\right) + \int_0^{H^*} dV'\right] \quad (15c)$$

The significance of eq 15b is that this mass balance involves the density which is based on the physical pore width, which is unambiguously defined. Another significant point is that the quantity required in the fitting is the amount introduced into the adsorption cell and it is always increasing with pressure. Therefore, we do not have any problem with the uncertainty of the maximum in the pore density excess. Thus, such a fitting is much more reliable than the fitting of the "indirectly" calculated excess quantity versus pressure (eq 11).

So the "direct conservation of mass" equation of the form of N versus pressure (eq 15b) involves the pore size distribution in the range from 0 to H*, $dV = f(H)\, dH$, the external surface area of the solid (S_{ext}), and the volume V''. Using the inversion method of optimization, such as the method of regularization, we can readily obtain the structural parameters of the solid as well as the void volume of the system. After we know these, the particle density can be readily computed from eq 15c.

After the pore size distribution has been obtained for pores having widths up to H^*, the internal geometrical surface area of these pores is calculated as (assuming slit shape)

$$S_{int} = \int_0^{H^*} \frac{2f(H)}{H}\, dH \quad (16)$$

Thus, the total geometrical surface area (S_{total}) is simply $S_{int} + S_{ext}$, and this value can be compared with the BET surface area (which is known not to represent the geometrical area).

4. Simulation Details

Simulations were performed for the adsorption of methane at 273.15 and 333.15 K in graphitic slit pores. The molecular model used for methane is a single site Lennard Jones model from Martin and Siepmann[17] with a collision diameter of 0.373 nm and interaction well depth of 148*k_b K (where k_b is Boltzmann's constant). The pores of the model activated carbon are treated as infinite slit pores. The potential energy between a pore wall and a fluid interaction site is calculated using the Steele potential.[18] The fluid−solid interaction parameters are obtained using the Lorentz−Berthelot mixing rule.[9]

Simulations were performed in the standard GCMC ensemble.[9] The simulation box was bounded in one direction by the finite width, H, of the pore and was given a box length in the remaining two directions of either 3.0 nm or 1.5 times the slit width (whichever was greater). Periodic boundary conditions were used in the lateral directions of the pore with fluid−fluid interactions having a lateral cutoff equal to half the simulation box length. Simulation pressures ranged from 0.05 to 20 000 kPa with the chemical potential set to that of methane according to an accurate equation of state.[19] The equilibrium period ranged between 3×10^6 to 150×10^6 attempted Monte Carlo moves depending on the number of particles in the simulation and the stage of adsorption. Collection of ensemble averages was conducted over a range of 3×10^6 to 30×10^6 attempted Monte Carlo moves, depending on the number of particles in the simulation. It was attempted, during the equilibration stage, to set the number of insertions such that a successful insertion was achieved, on average, every 5 attempted particle moves. This was not always possible, and where acceptance ratios of insertions were very low, the maximum number of insertions was set to 5 times the number of attempted moves.

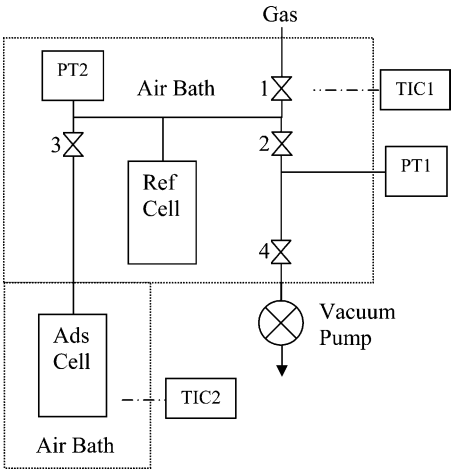

Figure 1. Experimental setup.

5. Results and Discussion

5.1. Experiment Results. To test the new method, the adsorption of methane up to 20 MPa was measured using a volumetric adsorption experiment. The experimental setup is shown in Figure 1.

The experiment setup consists of three parts. The first part is a low-pressure section, between valves 2 and 4, for vacuuming and adsorption pressure measurements below 130 kPa. The second part, between valves 1, 2, and 3, is a high pressure (to 20 MPa) reference volume. The final part is a high-pressure adsorption cell, downstream of valve 3. The first two sections are maintained at a constant temperature in an insulated, fan forced box. A Shimaden temperature controller (TC1 in Figure 1) is used to control the box temperature at 40.0 °C with a stability of 0.1 °C. The adsorption cell is placed within a fan-forced pipe within a tempering beaker. This ensures a very uniform temperature over the length of the adsorption cell. The temperature of the air forced past the adsorption cell is maintained at the adsorption

(17) Martin, M.; Siepmann, J. I. *J. Phys. Chem. B* **1998**, *102*, 2569.
(18) Steele, W. A. *Surf. Sci.* **1973**, *36*, 317.
(19) Setzmann, U.; Wagner, W. *J. Phys. Chem. Ref. Data* **1991**, *20*, 1061.

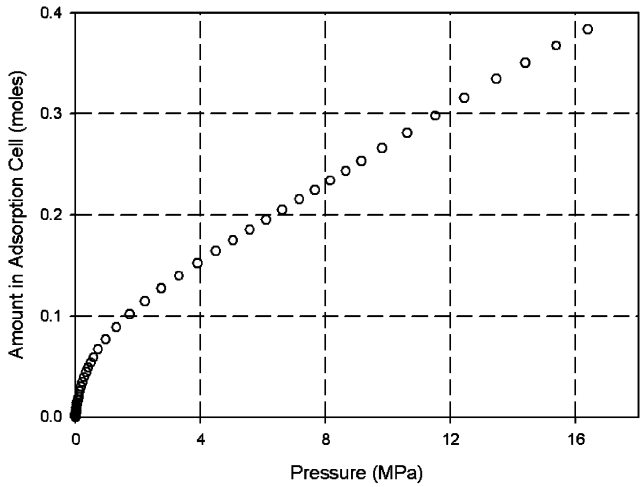

Figure 2. Total amount in the adsorption cell for experiment at 273.15 K.

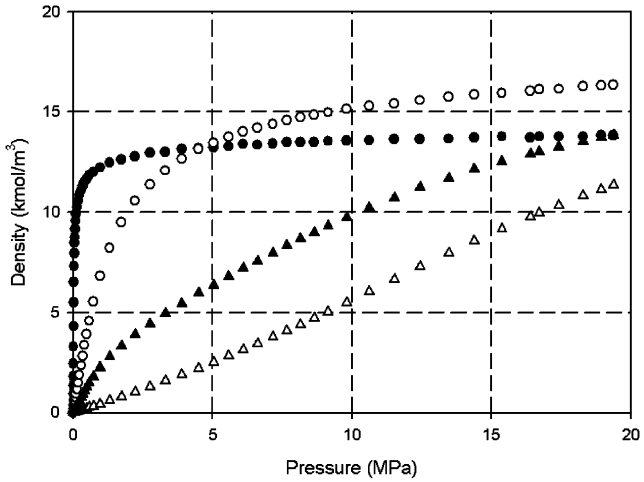

Figure 3. Absolute density of methane at 273.15 K in 0.733 nm pore (filled circles), 1.43 nm pore (empty circles) and 4.039 nm (filled triangles) from simulations and the bulk (empty triangles) from the equation of state. Pore densities are based on the physical pore width, H.

temperature given in the results. This temperature is controlled by a Julabo circulator with a stability of 0.01 °C. The adsorption cell is connected to the reference volume by 3 mm tubing to minimize the error caused by the temperature difference between the two sections. Experiment pressures below 130 kPa are measured by an MKS Baratron Transducer (PT1 in Figure 1) with an accuracy of 0.08% of reading. The internal volume of the transducer is controlled at 45 °C. Above 130 kPa, pressure is measured using a Druck Keller 33X pressure transmitter (PT2 in Figure 1) with an accuracy of 0.01% of full scale.

The activated carbon is evacuated for at least 48 h at 200 °C. After this, the adsorption cell is cooled to adsorption temperature under vacuum. The reference volume temperature is set to 40 °C. Temperatures are allowed to stabilize overnight under vacuum, and the experiment is ready to begin. Methane is dosed to the reference volume, and the pressure is recorded. The valve to the adsorption cell is opened and the pressure is observed. Once the pressure is deemed to be at equilibrium, the pressure is recorded, and the valve to the adsorption cell is closed. These steps are repeated until the maximum desired pressure is reached. Using this method, the total amount of methane in the experiment is always known unambiguously, since we know the volume, temperature, and pressure of the reference section. It follows

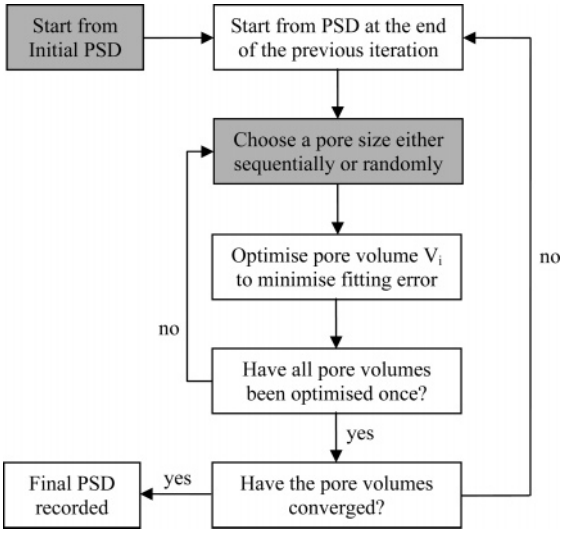

Figure 4. Process used for optimization of pore volumes.

Table 1. Summary of Results Derived from Different Methods of PSD Optimization

		physical properties of the system		
technique	property	all zero	$V_b = V_{He}$	N_2 PSD
forward sequential	V_μ (cc/g)	0.727	0.380	0.472
	S_{total} (m^2/g)	1129	993	1084
	V_b (cc)	21.09	31.13	26.25
	V_{cell} (cc)	30.76	36.18	32.52
	100Err	8.2	10.3	4.1
reverse sequential	V_μ (cc/g)	0.413	0.413	0.495
	S_{total} (m^2/g)	1083	1083	1105
	V_b (cc)	27.56	27.56	24.93
	V_{cell} (cc)	33.05	33.05	31.52
	100Err	13.6	13.6	3.9
random	V_μ (cc/g)	1.108	1.200	0.445
	S_{total} (m^2/g)	1352	1237	1069
	V_b (cc)	8.25	11.11	26.6
	V_{cell} (cc)	22.97	27.09	32.53
	100Err	25.1	15.2	3.1

then that the total amount downstream of valve 3 (i.e., the adsorption cell) is easily and unambiguously calculated. The experiment uses 13.3 g of Ajax activated carbon with a BET surface area of 1200 m^2/g. An example of an adsorption isotherm giving the total amount of methane in the adsorption cell as a function of equilibrium pressure is given in Figure 2.

5.2. Fitting Experiment Results Using the New Method. A series of GCMC simulations were completed for methane adsorption in slit pores from 0.733 to 4.665 nm. So the H^* in eqs 14−16 is 4.665 nm in this case. An additional simulation was performed in a pore whose width is 5.004 nm. The adsorption in the pore of 5.004 nm was considered to behave sufficiently like two independent surfaces to be able to use these results to calculate surface excess, $\Gamma(P)$. Some typical adsorption isotherms used for fitting the data are given in Figure 3.

With the collection of local isotherms from the simulations, we use MatLab optimization to match the theoretical results against the experimental data to determine the pore volumes, the external surface area (S_{ext}), and the bulk volume (V'). The fit of simulation to experiment data is defined by the error sum given in the equation below

$$\mathrm{Err} = \sum_{i=1}^{n} [\{(N_{ads}^i - N_{sim}^i)\}/\{N_{ads}^i\}]^2 \qquad (17)$$

Table 2. Plots of PSD Resulting from Different Optimization Methods and Initial Configurations[a]

Technique	Type of initial configuration		
	(A) All zero	(B) $V_b = V_{He}$	(C) N_2 PSD
(1) Forward sequential	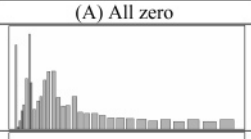	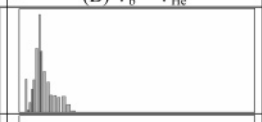	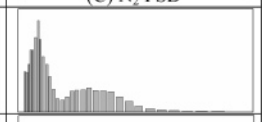
(2) Reverse sequential			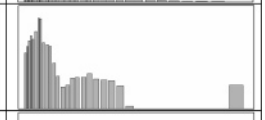
(3) Random			

[a] For all plots, the *y* axis is the pore volume per nanometer of pore width represented (in cc/g.nm) and the *x* axis is the pore size (in nm). The *y* scale of the different plots is variable but the *x* scale is consistent for all as 0.06−5.0 nm.

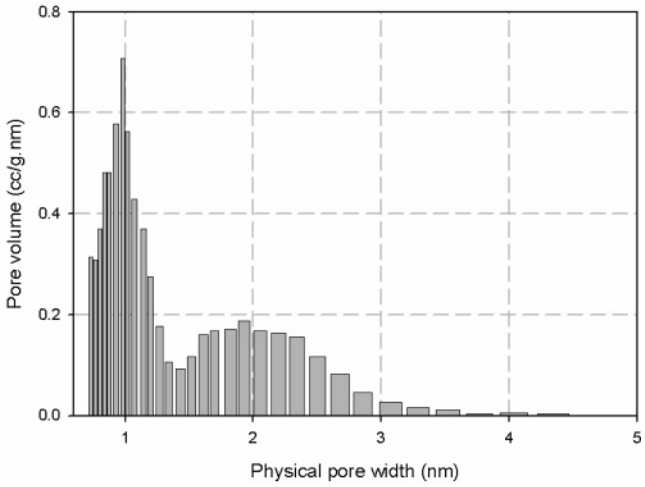

Figure 5. Pore size distribution resulting from the fitting of experimental data at 273.15 K using the forward sequential optimization method and an initial PSD from N_2 adsorption.

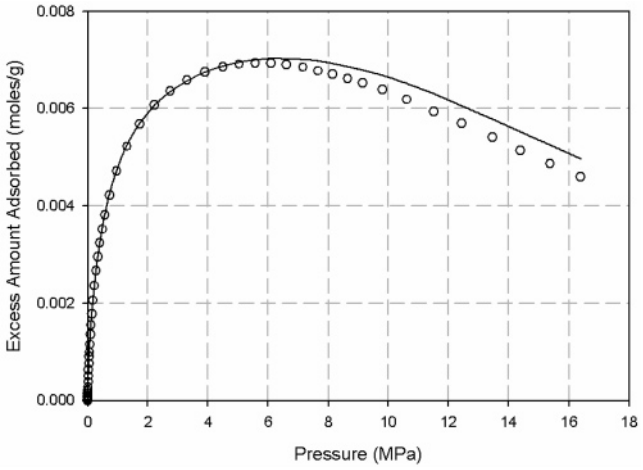

Figure 7. Excess amount adsorbed from experiment using the helium expansion volume (empty circles) and simulation (line) using the PSD in Figure 5.

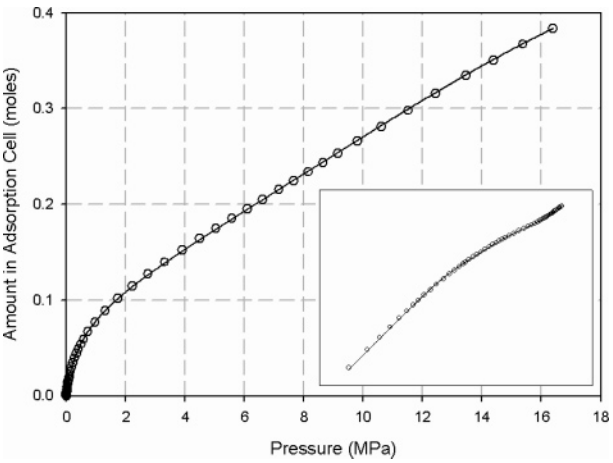

Figure 6. Amount in adsorption cell at 273.15 K, from experiment (empty circles) and simulation (line) using the PSD in Figure 5. Inset is the same plot in a log−log scale to show details at low pressure.

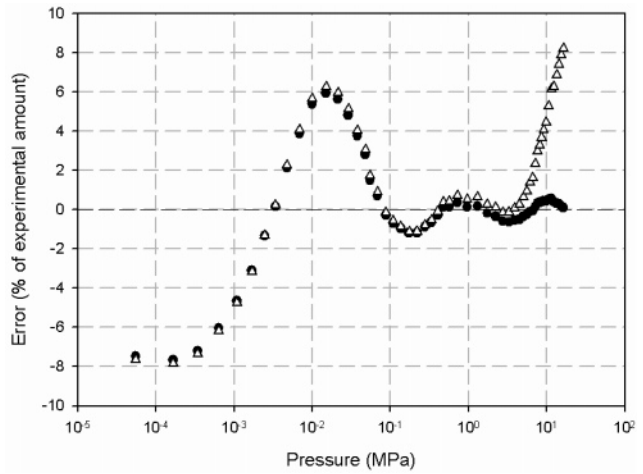

Figure 8. Difference between simulation, using the PSD in Figure 5, and experiment for the absolute amount in the adsorption cell (filled circles) and the excess amount adsorbed (empty triangles) at 273.15 K.

where Err is the error sum to be minimized when fitting the experimental data, n is the number of isotherm points N^i_{ads} is the amount in the adsorption cell from experiment, and N^i_{sim} is the amount in the adsorption cell from simulation according to eq 14. Now the fitting of the isotherms, from GCMC, to the experimental data is a very ill posed optimization problem. There are numerous solutions giving very similar fits and it is very difficult to identify local and global minimum in the error sum, Err. The PSD obtained depends on the optimization technique and the starting PSD used. The optimization process used is best described by a flowchart and this is given in Figure 4.

So the optimization is an iterative process of optimizing the fit between simulation and experimental data (i.e. minimizing Err in eq 17) by one pore volume at a time. In Figure 4, shaded

boxes indicate steps that vary between different types of optimization. The types of initial PSDs considered are: (1) All volumes, and external surface area, set to zero. (2) All pore volumes and surface area set to zero and the bulk volume assigned as equal to the volume from helium expansion. (3) Set to the PSD and surface area calculated from N_2 adsorption at 77 K using DFT. The bulk volume is set to a value inferred from helium expansion and the N_2 PSD.

The choice of the pore or external surface area or bulk volume to be optimized is made by one of the following methods: (1) Choosing the pore size sequentially from the pore size of 0.733 to 4.665 nm, followed by external surface area and then bulk volume. This is termed hereafter as "forward sequential"; (2) Choosing the pore size sequentially from bulk volume to external surface area to pore sizes from 4.665 to 0.733 nm. This is termed as "reverse sequential". (3) The pore is chosen randomly from a list of pores which have not been optimized yet in that iteration.

Now using the methods described above we can calculate a series of PSDs. The major features of these PSDs are summarized in Table 1, and the PSD generated are given in Table 2. Note that V' is the total free volume of the cell (including pore and bulk volume), V_μ is the micropore volume (pores < 5.0 nm) of the adsorbate on a per gram basis (13.3 g of activated carbon used), V_b is the bulk volume defined as $V' - m_p V_\mu$, and S_{total} is the total surface area.

Tables 1 and 2 show wild variability in the PSDs obtained between the different types of optimization. The best fits and the most realistic PSDs are achieved when the optimization is started from the reasonable guess of the N_2 PSD. Without this reasonable initial guess, the PSDs achieved bear little resemblance to that expected and give relatively poor fits to the experimental data. Also, physically impossible configurations are generated with the micropore and adsorption cell volumes being either impossibly high (higher than that measured by helium expansion of 33.0 cm^3) or impossibly low (the volume should not be less than 32.0 cm^3). It must be emphasized that no restrictions were placed on the pore volumes for the optimization. Micropore volumes (V_μ) also vary to a large degree from 0.445 to 1.200 cm^3/g when values should fall within the range from 0.4 to 0.5 cm^3/g. Surface areas are considerably more consistent ranging from 993 to 1352 m^2/g. These compare reasonably well with the BET surface area of 1200 m^2/g. However, the expectation is that the geometric surface area should be less than this and is only exceeded by PSDs with an unreasonably high micropore volume. So the best fit is provided by starting from the N_2 PSD. The PSD achieved starting from the N_2 PSD and using the forward sequential method is plotted in Figure 5 to more clearly show the features of this PSD. This PSD will be used for further discussion in this paper.

The PSD in Figure 5 results in one of the best fits to the experimental data. The comparison between simulation and experiment for the amount of methane in the adsorption cell is made in Figure 6.

The fit to the data is very good, with almost imperceptible differences at high pressure and small differences at low pressure. Now a comparison can be made between the excess calculated from experimental data using the helium expansion volume and that calculated as the excess from the simulation data (i.e., the first two terms in eq 14).

So the experimental and simulation excess amounts adsorbed become significantly different in the high-pressure region. Below about 4MPa, the differences are very small. The difference between the simulation and experiment for both the amount in the adsorption cell and the excess amount adsorbed is given in Figure 8.

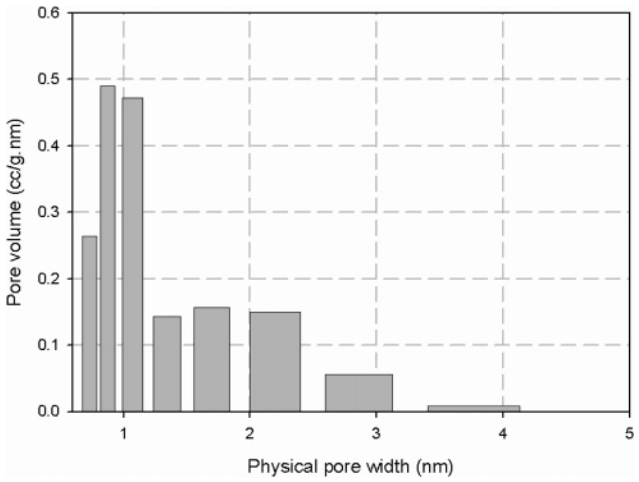

Figure 9. PSD from fitting only 8 pore volumes to the experimental data at 273.15 K.

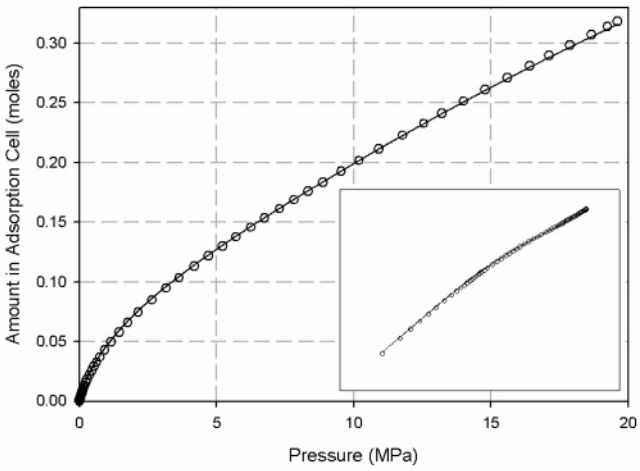

Figure 10. Amount in adsorption cell at 333.15 K, from experiment (empty circles) and simulation (line) using the PSD in Figure 5. Inset is the same plot in a log−log scale to show details at low pressure.

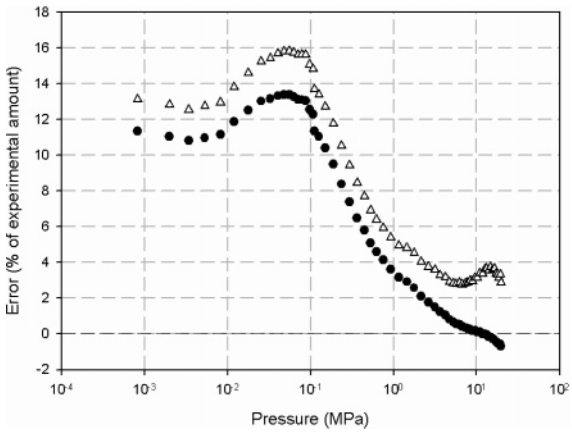

Figure 11. Difference between simulation, using the PSD in Figure 5, and experiment for the absolute amount in the adsorption cell (filled circles) and the excess amount adsorbed (empty triangles) at 333.15 K.

The multiple types of PSD obtained in Table 2, even for the same type of initial configuration, suggests that experimental data can be fitted with considerably fewer pore sizes than the 32 originally used. To test this, the PSD was determined again

using one-quarter as many pore sizes. The optimization was completed using pores selected by the forward sequential method and starting from the N_2 PSD (adjusted for the smaller number of pores). This optimization process resulted in the PSD given in Figure 9.

The PSD in Figure 9 is still very similar to that in Figure 5 for the much larger number of pores. It is approximately bimodal with peaks at about 1 and 2 nm. It also gives nearly the exact same properties for the adsorption system with, $V_\mu = 0.469$ cm^3/g, $S_{total} = 1071$ m^2, $V_b = 26.26$ cm^3, and $V_{cell} = 32.50$ cm^3. Somewhat surprisingly, the fit for this system with fewer pores is even better (having a percentage error of 2.2%). The prediction of the experimental data is near identical to that in Figures 6 and 7, with the error having a similar form to Figure 8 but with a slightly lower magnitude. Given the similarities, these results are not shown for brevity. So the resolution achievable using only supercritical data is not very good. With the PSD gained using the data 273.15 K, it should be possible to predict the adsorption at another temperature. To this means, equivalent experiments and simulations were performed at 333.15 K. The fit between the experiment and simulation, using the PSD in Figure 5, is given in Figure 10.

So the fit appears to be quite good, with the high pressure behavior predicted very well. This would indicate that the PSD used and the estimate of the bulk volume gives a good estimate of the "free" volume of the system. The accuracy of the prediction at low pressure is best visualized with an error plot. This is done in Figure 11.

So the fit at low pressure is much poorer than that at higher pressures. This seems to indicate a discrepancy in the fluid−solid interaction model, most particularly in the micropore range. An attempt was made to optimize the PSD to fit both the data at 273.15 and 333.15 K, but the fit for the 333.15 was only marginally improved. The inability to fit a PSD for the two sets of data together, even for easily fitted super critical adsorption again demonstrates some inadequacy in the model. This would require quite considerable additional experimental and simulation work to (even possibly) resolve.

6. Conclusions

We have presented in this paper a new method to determine micropore size distribution by using adsorption data of methane in activated carbon under supercritical conditions. This new method requires only information of the amount of methane loaded into the adsorption cell and the equilibrium pressure at the end of each dose and removes the need of determining the void volume. However, the approach requires a good initial estimate of the PSD. Generating a PSD without such an initial guess was found to be extremely unreliable. Future improvement of the determination of PSD seems to lie in using both sub-critical and supercritical data. The adsorption of a PSD from one temperature, 273.15 K, to another, 333.15 K, was found to give a reasonable prediction of adsorption at moderate to high pressure but significantly over predicted the adsorption at low pressure.

Acknowledgment. This work is supported by the Australian Research Council.

Appendix 1. Helium Expansion Method

Let V be the volume of the adsorption cell. This volume is the sum of the bulk volume outside the particle (V_b), the pore volume (V_p), and the solid volume (V_s)

$$V = V_b + V_p + V_s$$

The void volume is the sum of the first two terms in the right-hand side of the above equation. By expanding helium from a reservoir of known volume V_0 and a pressure P_0 into the adsorption cell, we have the following conservation of mass for this process of expansion

$$NR_gT = P_0V_0 = P_\infty V_0 + P_\infty V_b + P_\infty V_p^{(1)} + N_{ads}R_gT \quad \text{(A1.1)}$$

where $V_p^{(1)}$ is the void volume within the particle that is occupied by free molecule. The remaining void volume $V_p^{(2)}$ is occupied by the adsorbed molecules. Because the density of adsorbed molecule is much greater than the density in the bulk phase, we have the following inequality relation:

$$N_{ads}R_gT \gg V_p^{(2)}P_\infty \quad \text{(A1.2)}$$

Very often the critical assumption made by many is that helium does not adsorb in pores, and in so doing the mass balance equation becomes

$$NR_gT = P_0V_0 = P_\infty V_0 + P_\infty V_b + P_\infty V_p^{He} \quad \text{(A1.3)}$$

from which we can calculate the void volume as measured by helium expansion

$$V_b + V_p^{He} = \frac{V_0(P_0 - P_\infty)}{P_\infty} \quad \text{(A1.4)}$$

However, in case of adsorption, we can see from eqs A1.1 and A1.2 that if we use eq A1.4 to calculate the void volume we would over-estimate the actual pore volume. One possible way of obtaining the correct void volume is to calculate the apparent void volume from eq A1.4 for a range of temperature and then plot this apparent void volume versus the inverse of temperature. Extrapolation of this curve to $1/T = 0$ (i.e., the void volume axis) would yield the "true" void volume. It should be remembered that this void volume as measured by helium, V_p^{He}, is not necessarily the same as the void volume for arbitrary adsorbate.

Appendix 2. Relationship between the Physical, *H*, and Accessible, *H′*, Widths for a One-Site Model of Methane

H(A)	z_0 (A)	H'(A)	H(A)	z_0 (A)	H'(A)
6.5	2.9063	4.4174	17	3.0267	14.6766
7	2.9257	4.8786	17.5	3.0269	15.1762
7.5	2.9497	5.3306	18	3.0271	15.6758
8	2.9692	5.7916	18.5	3.0272	16.1756
8.5	2.9839	6.2622	19	3.0274	16.6752
9	2.9947	6.7406	19.5	3.0275	17.1750
9.5	3.0025	7.2250	20	3.0276	17.6748
10	3.0082	7.7136	21	3.0278	18.6744
10.5	3.0124	8.2052	22	3.0279	19.6742
11	3.0156	8.6988	23	3.0280	20.6740
11.5	3.0181	9.1938	24	3.0281	21.6738
12	3.0199	9.6902	25	3.0282	22.6736
12.5	3.0214	10.1872	26	3.0282	23.6736
13	3.0226	10.6848	27	3.0283	24.6734
13.5	3.0235	11.1830	28	3.0283	25.6734
14	3.0242	11.6816	29	3.0284	26.6732
14.5	3.0248	12.1804	30	3.0284	27.6732
15	3.0254	12.6792	50	3.0286	47.6728
15.5	3.0258	13.1784	80	3.0286	77.6728
16	3.0261	13.6778	∞	3.0286	
16.5	3.0264	14.1772			

Appendix 3. Second Integral in the Right-Hand Side of Equation 10

The second integral in the right-hand side of eq 10 is rewritten here for convenience.

$$\int_{H^*}^{\infty}\left[\rho_{av}(P;H) - \rho_b\left(\frac{H'}{H}\right)\right] dV \qquad \text{(A3.1)}$$

Note the limit of the integral is for pore widths greater than H^*, i.e., each of these pores large enough to behave like two independent surfaces. Since there is no overlap between the solid−fluid potential energies, adsorptions on these surfaces are practically the same. From the definition of the average pore density based on physical width, $\rho_{av} = \langle N\rangle/AH$, the above equation can be written as

$$\int_{H^*}^{\infty}\left[\frac{\langle N\rangle}{AH} - \rho_b\left(\frac{H'}{H}\right)\right] dV = \int_{H^*}^{\infty}\left[\frac{\langle N\rangle - \rho_b AH'}{2A}\right]\frac{2dV}{H} \qquad \text{(A3.2)}$$

The square bracket is simply the definition of the surface excess (mol/m^2), and since this surface excess is independent of pore width, the above equation will become

$$\Gamma(P)\int_{H^*}^{\infty}\frac{2dV}{H} \qquad \text{(A3.3)}$$

The integral of the above equation is simply the surface area contributed by large pores having width greater than H*. If this surface area is S_{ext}, the above equation is simply

$$\int_{H^*}^{\infty}\left[\rho_{av}(P;H) - \rho_b\left(\frac{H'}{H}\right)\right] dV = S_{ext}\Gamma(P) \qquad \text{(A3.4)}$$

LA061079+